Study of Monopulse-Antenna System for Angle Estimation in Analog Domain

Miroslav Hutár[1,*,†], Alejandro Gil-Martinez[2,†], José Antonio Lopez-Pastor[3,†], Peter Brida[1,†] and José L. Gómez Tornero[2,†]

[1]Department of Multimedia and Information-Communication, Technology University of Zilina, Zilina, Slovakia
[2] Department of Information and Communication Technologies, Technical University of Cartagena, Cartagena, Spain
[3]Department of Engineering and Applied Technologies ,University Center of Defense (CUD), San Javier Air Force Base, MDE-UPCT

Abstract

This paper investigates the advantages and drawbacks of using the amplitude monopulse technique to estimate the Direction of Arrival (DoA). The experimental setup consists of two-panel antennas and is utilized with three distinct tilting configurations to examine the effect on accuracy in estimating DoA. Experiments are done in an analog domain inside an anechoic chamber, and noise is applied to the results to simulate the effects of the real environment.

Keywords

amplitude monopulse technique, direction of arrival

1. Introduction

Localization is a critical aspect of IoT (Internet of Things) technology, as it enables devices to accurately determine their physical location in the world. This information is essential for a wide range of IoT applications, from healthcare [1] and asset tracking [2, 3] to agriculture [4]. In the field of wireless localization, the amplitude monopulse technique stands as one of the methods for direction finding [5, 6, 7]. This technique involves the utilization of two-panel antennas in the analog domain to generate multiple steering beams aimed at mirrored spatial angles. By employing separate antennas, the amplitude monopulse approach aims to achieve optimal conditions where these beams intersect perpendicularly at their Half-Power Beam Width (HPBW) point [8, 9, 10]. The amplitude monopulse technique has been widely investigated in recent years and integrated with several communication protocols for IoT applications, such as Bluetooth Low Energy (BLE) [11], Wi-Fi 2.4 GHz [7, 10, 12, 13] and Wi-Fi 5 GHz [8], RFID [9].

However, no one has dealt with the impact of different antenna tilting. It causes different beams crossover, which affects the accuracy of the amplitude monopulse technique for estimating the Direction of Arrival (DoA). In this paper, we investigate the impact of different antenna tilting and signal-to-noise ratio on direction-finding accuracy using the amplitude monopulse technique in the analog domain.

2. Amplitude-monopulse setup configuration

To analyze optimum design for monopulse antenna system, three distinct tilting angles are utilized. The setup of antennas is illustrated in Figure 1. Figure 1a shows tilting antenna under an angle $\alpha = 1°$. It corresponds to a cutoff point between two radiation patterns at perpendicular angle $\theta = 0°$. The

IPIN-WCAL 2025: Workshop for Computing & Advanced Localization at the Fifteenth International Conference on Indoor Positioning and Indoor Navigation, September 15–18, 2025, Tampere, Finland

*Corresponding author.
†These authors contributed equally.
miroslav.hutar@uniza.sk (M. Hutár); alejandro.gil@edu.upct.es (A. Gil-Martinez); joseantonio.lopez@cud.upct.es (J. A. Lopez-Pastor); peter.brida@uniza.sk (P. Brida); josel.gomez@ucpt.es (J. L. G. Tornero)
0000-0002-4505-1464 (M. Hutár); 0000-0001-7583-3224 (A. Gil-Martinez); 0000-0001-8474-1823 (J. A. Lopez-Pastor); 0000-0002-5442-9246 (P. Brida); 0000-0003-0488-3990 (J. L. G. Tornero)

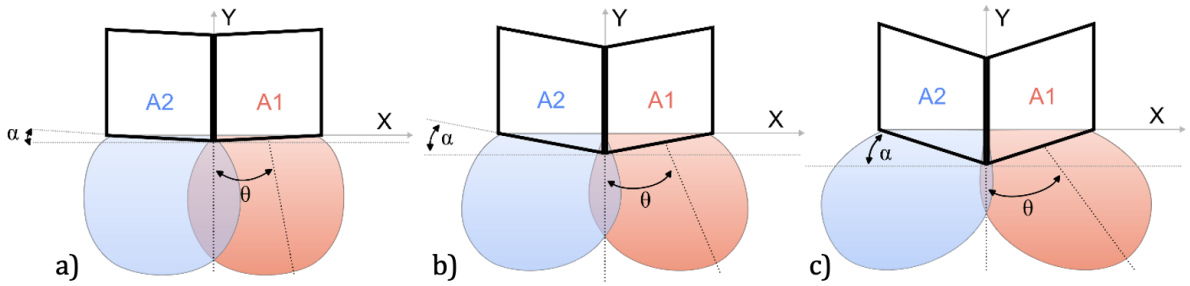

Figure 1: Two panel antennas in amplitude monopulse configuration with different tilting angles: a) $\alpha = 1°$, b) $\alpha = 6°$, c) $\alpha = 12°$.

second scenario is shown in Figure 1b. The tilted angle of the antenna is $\alpha = 6°$ and the crossover level of the main beams is -3 dB which is typically used for monopulse antenna systems [8, 9, 10, 14, 15]. The last scenario can be seen in Figure 2c. It is tilted under an angle $\alpha = 12°$ which produces a cutoff point at perpendicular angle at -6 dB. For our experiments, we used two-panel antenna of size 20cm × 20cm with 14 dBi peak gain. Because we want to study how our three scenarios will behave in the WiFi 2.4 GHz analog domain, a frequency of 2437 MHz, which corresponds to channel 6, was chosen.

The concept of a monopulse array utilizing two antennas is a configuration where two separate antennas are employed to generate two steering beams pointing in mirrored spatial directions. The beams are typically designed to intersect at a specific angle, such as the Half-Power Beam Width (HPBW) point, to optimize the accuracy of the direction estimation [8, 9, 10, 14, 15]. It corresponds to a cutoff point of -3 dB in the perpendicular angle $\theta = 0°$.

To obtain amplitude monopulse function from our measured amplitude of both beams in the whole angle $\theta = [-90°, 90°]$ we used formula [8, 9]

$$MF = \frac{\Delta_P(\theta)}{\Sigma_P(\theta)} = \frac{P_{A1}(\theta) - K_D \cdot P_{A2}(\theta)}{P_{A1}(\theta) + K_D \cdot P_{A2}(\theta)}, \tag{1}$$

where P_{A1} and P_{A2} is the received power of antenna A1 and antenna A2. Because antennas are not perfect, the gain patterns can be unbalanced, and it have to be corrected by correction factor K_D calculated as follows

$$K_D = \frac{P_{A1}(\theta = \theta°)}{P_{A2}(\theta = \theta°)} \rightarrow K_D(dB) = P_{A1}(\theta°) - P_{A2}(\theta°)(dB). \tag{2}$$

Analog measurements have been performed in the anechoic chamber at a radial distance of 3 m between transmitter and receiver, corresponding to the far-field region [14].

3. Analog measurements

The block diagram of the analog measurement setup is shown in Figure 2a. It consists of two-panel antennas and one reference antenna connected via coaxial cable to a vector network analyzer (VNA). Since VNA has only two ports, one is connected to a reference antenna, and only one of the two-panel antennas is measured at a time. So, measurements must be repeated for the second antenna of the two-panel antennas with the same conditions to obtain the monopulse pattern. VNA and turn table were connected to a PC with Matlab, which contains a script to control these devices. The whole setup is shown in Figure 2b. The purpose of analog measurement in the anechoic chamber is to determine how the radio signal behaves in optimal conditions (no reflection and multipath) and calibrate the radiation patterns for the amplitude-monopulse comparison technique [9].

The radiation patterns of the three different monopulse configurations are shown in Figure 3. The minimum tilting angle α is set to $1°$, which creates a crossover value between the two tilted beams of only -1 dB, as shown in Figure 1a. In such monopulse configurations, the closer the beams are, the

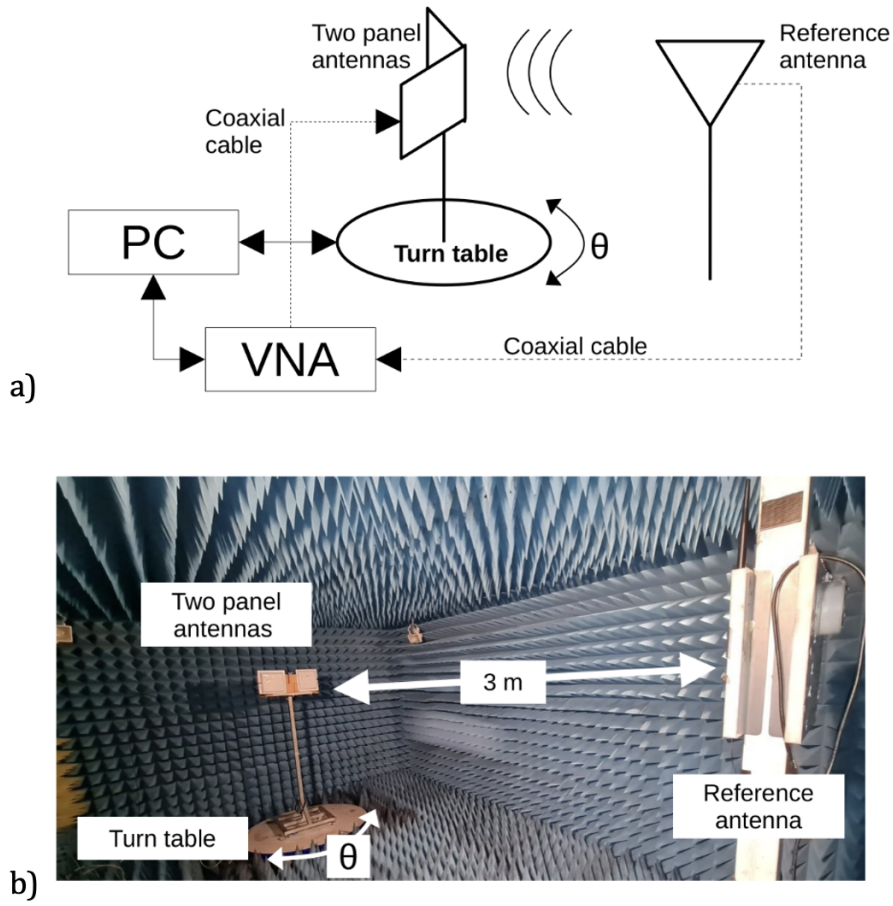

Figure 2: Analog measurements in anechoic chamber, a) schematic, b) real scenario.

higher the resulting Field of View (FoV), as demonstrated in Figure 4. Figure 3b presents the measured beams of the second tilted array configuration (see Figure 1b). In this case, the optimal monopulse configuration with -3 dB crossover level between adjacent beams -HPBW point according to (1)-, is obtained for a mechanical tilting angle of $\alpha = 6°$. Finally, Figure 3c shows the radiation pattern of the third tilted array configuration with the higher separation between beams (see Figure 1c). For this monopulse configuration, the beams intersect at a crossover level of -6 dB, which is the minimum overlapping as a result of the higher separation between beams. As it will be shown next, this reduces the FoV. The consequences of different tilting angles and associated crossover points can be evaluated by inspecting the monopulse functions MF (1), shown in Figure 4 for the three studied cases. As explained in [8], [9], the angular FoV without ambiguity is defined as the angular region in which the MF has a monotonous linear response, so that a unique DoA can be associated with any given value of the MF. In Figure 4, we can see how, for the configuration in which the beams are closer together (-1 dB crossover level), the slope of the linear MF is less steep, and therefore, an increment of the FoV is obtained. This can be seen in the red curve in Fig. 4, observing a wide FoV from $-31°$ to $31°$ for this tilting angle of $\alpha = 1°$. On the contrary, when the beams of the monopulse pattern intersect at lower crossover values, the slope of the MF is steeper, and the FoV is narrower. The lowest FoV from $-17°$ to $20°$ is achieved with the maximum tilting angle $\alpha = 12°$ corresponding to a crossover level of -6 dB (plotted with blue line).

At this point, one could think that the optimum monopulse antenna design is the one with the maximum FoV. However, if the slope of the MF is less steep, as it happens for the red MF in Figure 4, lower angular sensitivity for angle estimation is obtained. This will imply lower DoA accuracy, as will be shown with experiments.

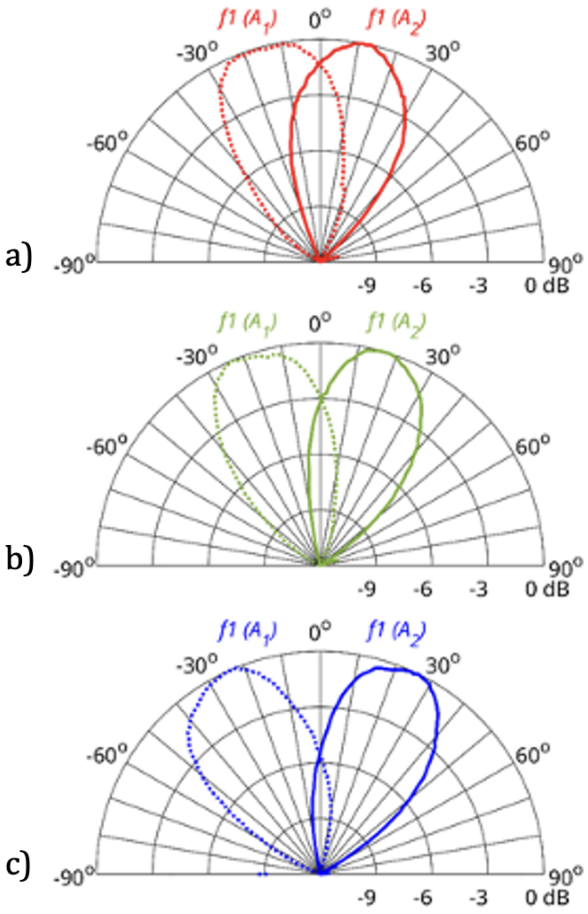

Figure 3: Analog measured radiation patterns in anechoic chamber for three amplitude monopulse configurations a) $\alpha = 1°$ b) $\alpha = 6°$ c) $\alpha = 12°$.

4. Direction finding estimation

Since the analog measurements were performed in an anechoic chamber (ideal environment), no noise or multipath effects were presented. To better evaluate the DoA estimation accuracy, the noise was

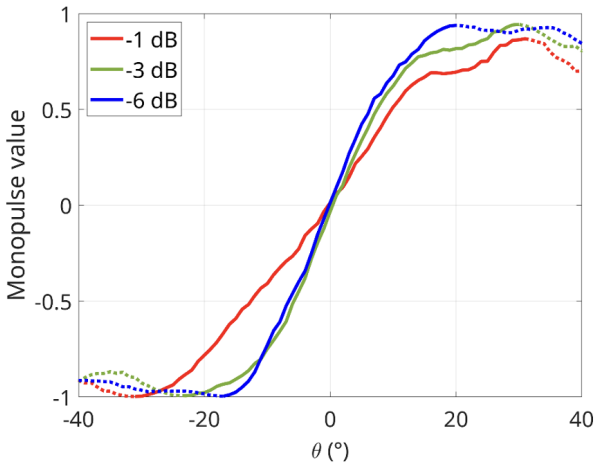

Figure 4: Analog-measured monopulse functions of the three antenna designs.

added to our measurements based on [16] for three signal-to-noise ratio (SNR) scenarios: 54, 64, and 74 dB. We create 100 samples of received power per degree for each tilted configuration and SNR. Then, the DoA was estimated using the same procedure described in [9]. The monopulse function for each antenna design shown in Figure 4 is used. Later, degree sample with noise is used for calculating monopulse value $MV(\theta)$ by the following formula

$$MV(\theta) = \frac{P_{A1} - K_D P_{A2}}{P_{A1} + K_D P_{A2}}, \tag{3}$$

afterwards the amplitude pseudospectrum $APS(\theta)$ is obtained by

$$APS(\theta) = -10 \cdot \log\left(\frac{1}{|MV(\theta) - MF|}\right). \tag{4}$$

The highest peak of $APS(\theta)$ inside FoV is estimated DoA. For the purpose of evaluate the performance, the DoA was calculated for each degree, antenna configuration, and SNR. Figure 5 shows the angular DoA estimation error for each SNR and tilted array configuration. Because FoV is a zone without ambiguities, the angle error outside of FoV increases. So, only angular error inside FoV was taken into account. As we can see, the DoA estimated error increases with lower SNR and decreases with higher SNR. This is due to the greater noise at lower SNR. As expected, the tilted array configuration with crossover -1 dB gains a higher error in DoA estimation than the configuration with a cutoff point of -6 dB. Due to less step in MF, little changes in received signal make a more varying highest peak in APS. The results of DoA estimation performance are summarized in Table 1. It compares different FoV with three SNR scenarios. The best results, a smaller DoA estimation error, are obtained with the tilted array

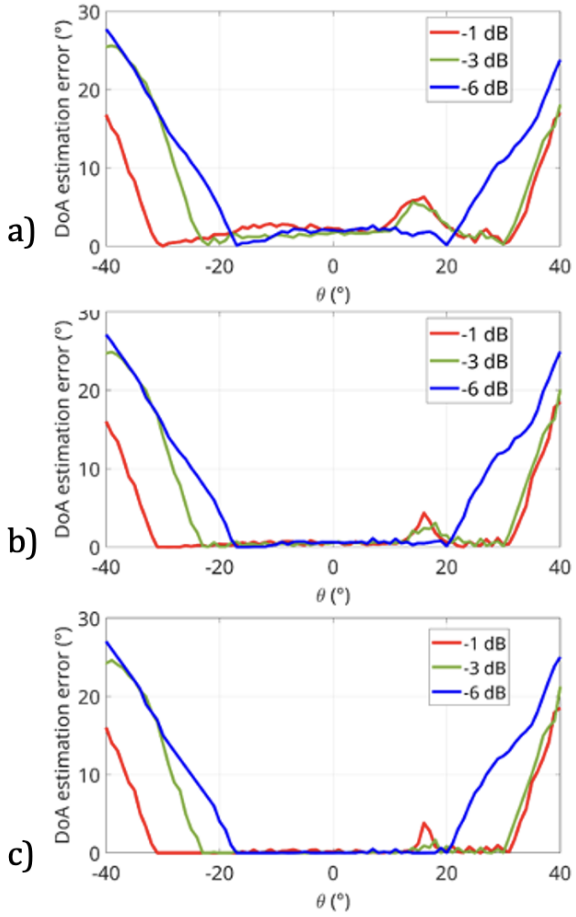

Figure 5: Analog DoA estimation error using amplitude monopulse technique for each tilted array configuration with SNR: a) 54 dB, b) 64 dB, c) 74 dB.

configuration of crossover point at -6 dB and the highest SNR 74 dB. The worst DoA estimation error was obtained with a tilted array configuration of -1 dB and the lowest SNR 54 dB. It is clearly visible in Figure 5.

5. Conclusions

This paper studied the impact of different tilting antenna array configurations for DoA estimation using the analog monopulse technique. Experiments were performed in an anechoic chamber to calibrate the system and obtain monopulse function. Subsequently, noise based on three different SNRs was applied to the measured data to simulate real environment signal changes. The results show that with a higher angle α we obtain a smaller FoV but the estimation of DoA is more accurate. On the other hand, with a lower angle α, the FoV is greater at the cost of lower precision in DoA estimation. SNR also has a significant impact on the accuracy of DoA estimation. The results are more accurate with higher SNR. Future work will focus on extending the study to real environment measurement, including the digital domain.

Acknowledgments

This work was supported in part by the Slovak Scientific Grant Agency (VEGA) Grant Agency through the Research of a Location-Aware System for Achievement of QoE in 5G and B5G Networks under Project 1/0588/22, and in part by the Spanish National projects TED2021-129196BC42 and PID2022-136590OB-C42.

Declaration on Generative AI

The author(s) have not employed any Generative AI tools.

References

[1] L. Bibbò, R. Carotenuto, F. Della Corte, An overview of indoor localization system for human activity recognition (har) in healthcare, Sensors 22 (2022). URL: https://www.mdpi.com/1424-8220/22/21/8119. doi:10.3390/s22218119.

[2] N. Karimpour, Z. Akusta Dagdevıren, V. Akram, O. Dağdeviren, A cloud-based asset tracking system for hospitals using ultra-wideband localization, Avrupa Bilim ve Teknoloji Dergisi (2021) 425–430. doi:10.31590/ejosat.960454.

[3] J. Machaj, P. Brida, S. Matuska, Proposal for a localization system for an iot ecosystem, Electronics 10 (2021). URL: https://www.mdpi.com/2079-9292/10/23/3016.

[4] M. Swain, M. F. Hashmi, R. Singh, A. W. Hashmi, A cost-effective lora-based customized device for agriculture field monitoring and precision farming on iot platform, International journal of communication systems 34 (2021).

[5] J. L. Gómez-Tornero, Smart Leaky-Wave Antennas for Iridescent IoT Wireless Networks, 2022, pp. 119–181. doi:10.1002/9781119813910.ch4.

[6] M. Passafiume, S. Maddio, G. Collodi, A. Cidronali, An enhanced algorithm for 2d indoor localization on single anchor rssi-based positioning systems, in: 2017 European Radar Conference (EURAD), 2017, pp. 287–290. doi:10.23919/EURAD.2017.8249203.

[7] J. A. López-Pastor, M. Poveda-García, A. Gil-Martínez, D. Cañete-Rebenaque, J. L. Gómez-Tornero, 2-d localization system for mobile iot devices using a single wi-fi access point with a passive frequency-scanned antenna, IEEE Internet of Things Journal 10 (2023) 14995–15011. doi:10.1109/JIOT.2023.3262830.

[8] A. Gil-Martínez, M. Poveda-García, J. A. López-Pastor, J. C. Sánchez-Aarnoutse, J. L. Gómez-Tornero, Wi-fi direction finding with frequency-scanned antenna and channel-hopping scheme, IEEE Sensors Journal 22 (2022) 5210–5222. doi:10.1109/JSEN.2021.3122232.

[9] J. L. Gómez-Tornero, D. Cañete-Rebenaque, J. A. López-Pastor, A. S. Martínez-Sala, Hybrid analog-digital processing system for amplitude-monopulse rssi-based mimo wifi direction-of-arrival estimation, IEEE Journal of Selected Topics in Signal Processing 12 (2018) 529–540. doi:10.1109/JSTSP.2018.2827701.

[10] M. Poveda-García, J. A. López-Pastor, A. Gómez-Alcaraz, L. M. Martínez-Tamargo, M. Pérez-Buitrago, A. Martínez-Sala, D. Cañete-Rebenaque, J. L. Gómez-Tornero, Amplitude-monopulse radar lab using wifi cards, in: 2018 48th European Microwave Conference (EuMC), 2018, pp. 464–467. doi:10.23919/EuMC.2018.8541674.

[11] S. Matuska, J. Machaj, M. Hutar, P. Brida, A development of an iot-based connected university system: Progress report, Sensors 23 (2023). URL: https://www.mdpi.com/1424-8220/23/6/2875. doi:10.3390/s23062875.

[12] A. Cidronali, G. Collodi, M. Lucarelli, S. Maddio, M. Passafiume, G. Pelosi, S. Selleri, Improving phaseless direction of arrival estimation exploiting space and frequency diversities, in: 2019 16th European Radar Conference (EuRAD), 2019, pp. 49–52.

[13] M. Poveda-García, D. Cañete-Rebenaque, J. L. Gómez-Tornero, Frequency-scanned monopulse pattern synthesis using leaky-wave antennas for enhanced power-based direction-of-arrival estimation, IEEE Transactions on Antennas and Propagation 67 (2019) 7071–7086. doi:10.1109/TAP.2019.2925970.

[14] J. A. López-Pastor, A. Gómez-Alcaraz, D. Cañete-Rebenaque, A. S. Martinez-Sala, J. L. Gómez-Tornero, Near-field monopulse doa estimation for angle-sensitive proximity wifi readers, IEEE Access 7 (2019) 88450–88460. doi:10.1109/ACCESS.2019.2925739.

[15] J. A. López-Pastor, P. Arques-Lara, J. J. Franco-Peñaranda, A. J. García-Sánchez, J. L. Gómez-Tornero, Wi-fi rtt-based active monopulse radar for single access point localization, IEEE Access 9 (2021) 34755–34766. doi:10.1109/ACCESS.2021.3062085.

[16] M. D. Sacchi, Adding noise with a desired signal-to-noise ratio, https://sites.ualberta.ca/~msacchi/SNR_Def.pdf/, 2008. [Online; accessed August-2025].